JOURNAL OF MATERIALS SCIENCE 17 (1982) 3197–3203

A simplified method of generating layer sequences for SiC polytypes

Part 2 *Application to the determination of new polytypes $20H_{(a)}$ and $20H_{(b)}$*

ZENZABURO INOUE, YOSHIZO INOMATA, HIROKICHI TANAKA
National Institute for Research in Inorganic Materials, Namiki 1-1, Sakura-mura, Niihari-gun, Ibaraki 305, Japan

HIROSHI KOMATSU
Research Institute for Iron, Steel and Other Metals, Tohuku University, 1-1 Katahira 2-chome, Sendai 980, Japan

New polytypes of silicon carbide, $20H_{(a)}$ and $20H_{(b)}$, have been synthesized in a very pure graphite crucible reacted with molten silicon at 2000 and 2300° C, respectively. A simplified method for generating the layer sequences has been applied to the determination of their crystal structures. The polytypes of $20H_{(a)}$ and $20H_{(b)}$ are successfully revealed by this method to be (44222222) and (32322323), respectively.

1. Introduction

About 160 polytypes of silicon carbide have been reported to date, and layer structures have been assigned to about half of these [1–4]. As an addition to these, two new polytypes, $20H_{(a)}$ and $20H_{(b)}$, are reported in this paper. Their layer structures have been successfully revealed by the application of a "simplified method" [5] on the basis of the principle that SiC polytypes of high-temperature phases will not have Zhdanov number "1" in their layer sequences [6–11]. The layer sequences of $20H_{(a)}$ and $20H_{(b)}$ can be represented as (44222222) and (32322323), respectively. Although crystal symmetry of both polytypes belong to $P3m1$, they produce an X-ray diffraction pattern of $6/mmm$. They are typical examples of diffraction enhancement of symmetry [12], and are the second existing examples following 10H [13] to have been reported so far in the matter of diffraction enhancement of symmetry of SiC polytypes [14–16].

2. Experimental details

A new polytype, $20H_{(a)}$, was grown together with many SiC crystals, mostly 4H, in a very pure graphite crucible at 2000° C for 2 h by the molten silicon method [17]. Another new polytype, $20H_{(b)}$, was obtained together with many others, mostly 6H and 15R, under a condition rich in silicon vapour [18] at 2300° C for 2.5 h. The ash content of the graphite crucible used for both experiments was less than 20 ppm and the purity of the silicon powder used as the starting material was better than 99.999%.

The external form of $20H_{(a)}$ is a hexagonal frustum and is 0.2 mm diameter as shown in Fig. 1. The form of $20H_{(b)}$ is approximately a hexagonal prism, 0.4 mm diameter and 1.2 mm long along the c-axis as shown in Fig. 2. The colour of these crystals was pale green in transmitted light.

In order to examine the syntactic coalescence and to analyse the layer structure of both crystals, X-ray oscillation photographs about the c-axis were taken of the upper and lower halves of each specimen with CuKα radiation.

Their $10\bar{1}\cdot l$ row reflection spots are given in Figs. 3 and 4. Fig. 3a, which was obtained from the upper part of $20H_{(a)}$, indicates that the reflec-

0022–2461/82/113197–07$03.34/0

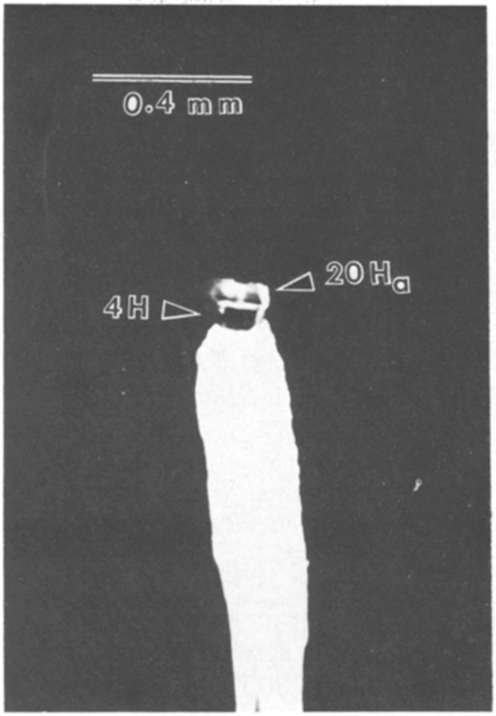

Figure 1 A photograph of $20H_{(a)}$ coalescing with 4H.

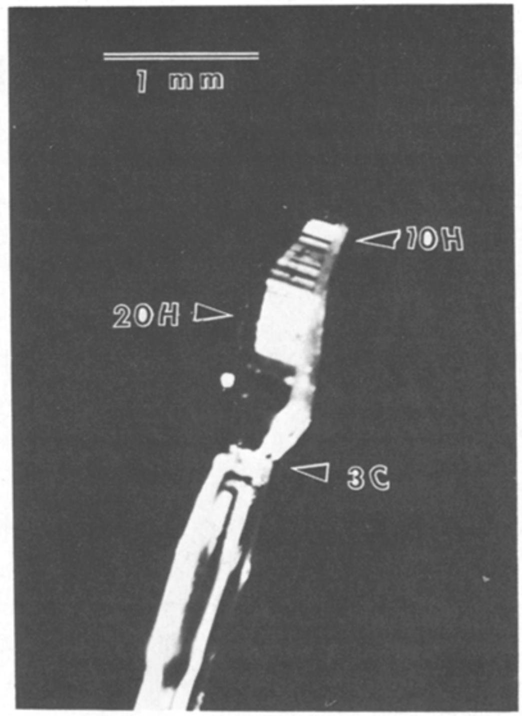

Figure 2 A photograph of $20H_{(b)}$ coalescing with 10H and 3C.

tion spots are only those of the $20H_{(a)}$ polytype. Fig. 3b, obtained from the lower part of $20H_{(a)}$, shows only those of 4H. From these results, it is clear that $20H_{(a)}$ and 4H polytypes coalesce into one crystal with their c-axes in parallel to each other, and that $20H_{(a)}$ is in the upper part of the crystal while 4H is in the lower part as shown by the arrows in Fig. 1.

On the other hand, Fig. 4a and b, from the upper and the lower parts of $20H_{(b)}$, respectively, show the reflection spots of 10H only and $20H_{(b)}$ mixed with those of 3C. Furthermore, 3C reflection spots were found to be predominant in the diffraction pattern of the bottom part. From these results, it was confirmed that 10H, $20H_{(b)}$ and 3C coalesce into one crystal with their c-axes parallel, and that 10H and 3C grew in the upper part and at the bottom of the crystal, respectively, and $20H_{(b)}$ is sandwiched between them as shown by the arrows in Fig. 2.

3. Surface observations

In order to analyse the growth mechanisms of $20H_{(a)}$ and $20H_{(b)}$, phase-contrast microscopic techniques and multiple-beam interferometric measurements were made on their (0001) surfaces.

Fig. 5 is a positive phase-contrast photograph of the $20H_{(a)}$ crystal, which shows a polygonal spiral originated from a single screw dislocation centre. The straightness of growth steps proves that this crystal has grown in a state of low supersaturation at 2000° C. The step height of this hexagonal spiral was measured to be about 5 nm by the multiple-beam interferometry, whose value coincides with the c-period determined by the X-ray method. This single-centred spiral with the height of a unit cell is evidence that the origin of the polytype is due to a screw dislocation [19].

In the case of $20H_{(b)}$, unfortunately, we could not observe the (0001) surface, because the crystal was sandwiched between 10H and 3C. Nevertheless, because of the sharp diffraction spots of $20H_{(b)}$, we inclined to adopt the screw dislocation mechanism for the growth of this polytype.

It is conjectured that $20H_{(b)}$ has grown out of the mother crystal of 3C, which always grows at the initial stage [20], and disappears at the later stage at 2300° C as a result of thermal etching. Evidence of thermal etching may be seen on the bottom surface of this crystal as shown

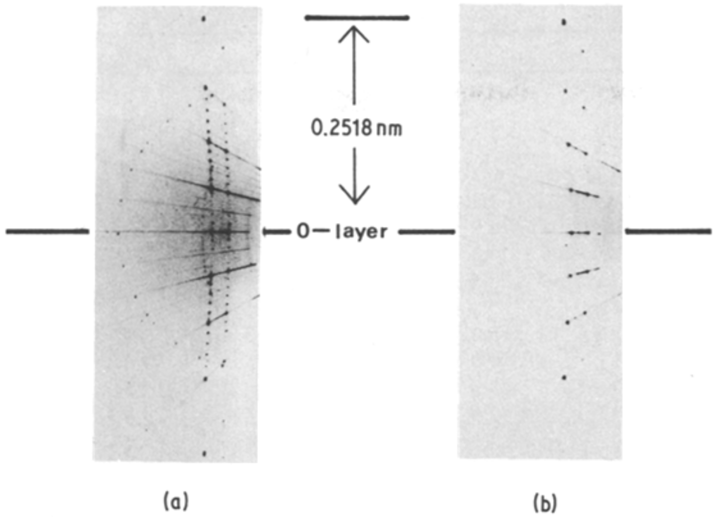

Figure 3 The reflection spots of the $10\bar{1}\cdot l$ row in the c-axis oscillation photographs of $20H_{(a)}$ coalescing with 4H type. (a) Reflection spots of $20H_{(a)}$; (b) those of 4H only.

in Fig. 6. It is clear in this positive phase-contrast photomicrograph that the bottom surface exhibits linear grooves intersecting each other at 60° (or 120°) and concave steps characteristic of weak thermal etching on 3C crystals.

4. Structure determination

It is obvious from the X-ray oscillation photographs of $20H_{(a)}$ and $20H_{(b)}$ shown in Figs. 3 and 4 that both photographs are mirror-symmetric about the zero-layer line with respect to position and intensity of X-ray reflections. Their X-ray diffraction patterns give the symmetry of $6/mmm$. Therefore, their structure might be supposed to be hexagonal symmetry at first glance. The possible layer sequences of 20-layered hexagonal structure are derived from the "simplified method" described in the previous paper (Part 1) as follows:

$$10\cdot 10, 622622, 532532, 442442, 433433.$$

We then calculated the periodic intensity distribution function S which is characteristic of the layer sequence of SiC polytypes [21]. S is given as

$$S(hkl) = \frac{F(hkl)}{f_0(hkl)}$$

where $F(hkl)$ is the structure factor of the SiC polytype, and $f_0(hkl)$ is the Fourier transform of the single SiC layer. Each of the $S_{0\cdot 1-5}$ calculated for the $10\bar{1}\cdot l$ row of each of the five hexagonal layer sequences mentioned above, was compared with $S_{0\cdot a}$ and $S_{0\cdot b}$ which corresponded to the S value observed over the $10\bar{1}\cdot l$ rows of $20H_{(a)}$ and $20H_{(b)}$.

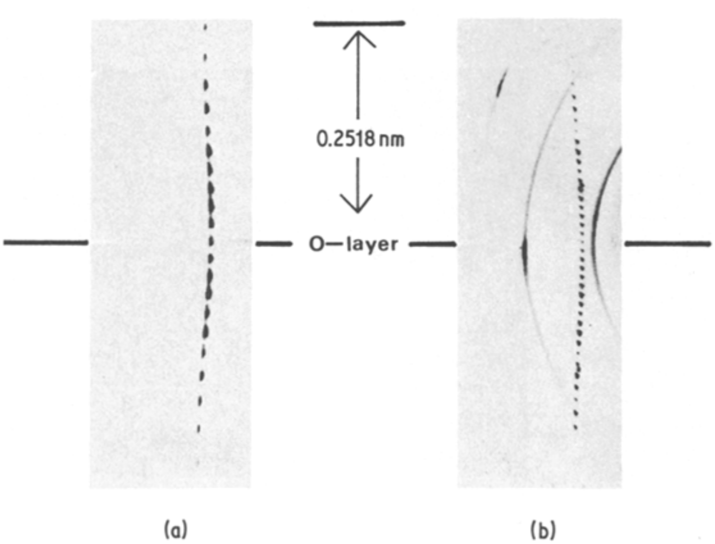

Figure 4 The reflection spots of the $10\bar{1}\cdot l$ row in the c-axis oscillation photographs of $20H_{(b)}$ coalescing with 10H and 3C types. (a) reflection spots of 10H only; (b) those of $20H_{(b)}$ and 3C superimposed.

TABLE I Observed S_0 and calculated S_c values for the $1 0 \bar{1} \cdot l$ reflections of $20H_{(a)}$ and $20H_{(b)}$

$10\bar{1}\cdot l$	$S_{o\cdot a}$	$S_{o\cdot b}$	S_{c1}	S_{c2}	S_{c3}	S_{c4}	S_{c5}	S_{c6}	S_{c7}	S_{c8}
0	3.8	1.3	1.0	1.0	1.0	2.0	1.0	2.0	1.0	1.0
1	1.9	1.4	0.6	2.5	1.6	1.6	0.1	1.0	0.6	1.4
2	1.0	2.8	1.2	1.2	1.2	1.9	1.9	1.6	0.9	1.5
3	0.2	3.0	0.8	0.2	3.1	0.3	2.3	0.5	2.8	0.7
4	1.2	2.6	1.9	1.9	1.9	1.2	4.9	2.0	2.5	0.9
5	7.9	4.7	1.7	5.2	3.9	6.9	1.7	3.5	3.0	6.2
6	2.7	6.7	7.9	7.9	7.9	4.9	5.9	8.3	6.4	4.0
7	4.3	3.9	9.9	2.3	3.9	3.8	8.9	6.1	9.4	8.7
8	4.2	3.0	4.9	4.9	4.9	7.9	1.9	6.6	2.5	6.4
9	4.4	6.1	1.9	8.1	7.9	5.0	4.2	3.1	5.4	4.4
10	10.3	10.0	3.0	3.0	3.0	6.0	9.0	6.0	4.6	3.0
11	4.7	5.5	1.9	8.1	7.9	5.0	4.3	3.1	5.4	4.4
12	4.6	2.1	4.9	4.9	4.9	7.9	1.9	6.6	2.6	6.4
13	3.4	3.6	9.9	2.3	3.9	3.8	8.9	6.1	9.4	8.6
14	2.4	6.4	7.9	7.9	7.9	4.9	4.9	8.3	6.4	4.0
15	8.3	5.4	1.7	5.2	3.9	6.9	1.7	3.5	3.0	6.2
16	0.2	3.1	1.9	1.9	1.9	1.2	4.9	2.0	2.5	0.9
17	0.8	3.4	0.8	0.2	3.1	0.3	2.3	0.5	2.8	0.7
18	1.4	3.0	1.2	1.2	1.2	1.9	1.9	1.6	0.9	1.5
19	1.8	2.2	0.5	2.4	1.6	1.6	0.1	1.0	0.6	1.4
20	3.9	1.5	1.0	1.0	1.0	2.0	1.0	2.0	1.0	1.0
Model	–	–	(10.10)	(622622)	(532532)	(442442)	(433433)	(8822)	(7733)	(6644)
RA(%)	–	–	82.1	61.5	66.0	36.4	77.3	63.0	77.7	48.8
RB(%)	–	–	68.2	45.7	36.5	46.3	47.2	52.4	39.2	60.6

We here define the reliability index R as follows:

$$R_n(\%) = \frac{\sum ||S_0| - |S_{c\cdot n}||}{\sum |S_0|} \times 100, \qquad (2)$$

where n is the reference number for one of the 5-layer sequences. The values of RA_n and RB_n were derived by replacing S_0 with $S_{0\cdot a}$ and $S_{0\cdot b}$ in Equation 2. These $S_{c\cdot 1-5}$, $S_{0\cdot a}$, $S_{0\cdot b}$, RA_{1-5} and RB_{1-5} values are presented in Table I.

Upon examining these results, it will be noticed that none of the calculated $S_{c\cdot 1-5}$ values of 5-layer sequences gives a good agreement with $S_{0\cdot a}$ and $S_{0\cdot b}$. The minimum values of RA and RB are 36.4% for (424424) and 36.5% for (532532) sequences, respectively. These values are too large to conclude that the layer structures of $20H_{(a)}$ and $20H_{(b)}$ may be assigned to (424424) and (532532), respectively. Therefore, it was concluded that it would be necessary to look for another possibility other than hexagonal structure.

Ramsdell and Kohn [13] reported in 1951 that 10H SiC polytype with layer sequence 3223 gives

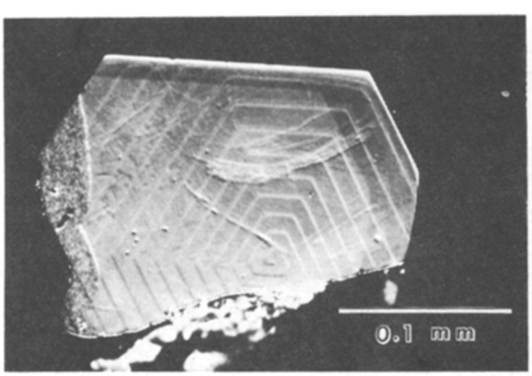

Figure 5 Positive phase-contrast photograph of (0 0 0 1) surface of $20H_{(a)}$.

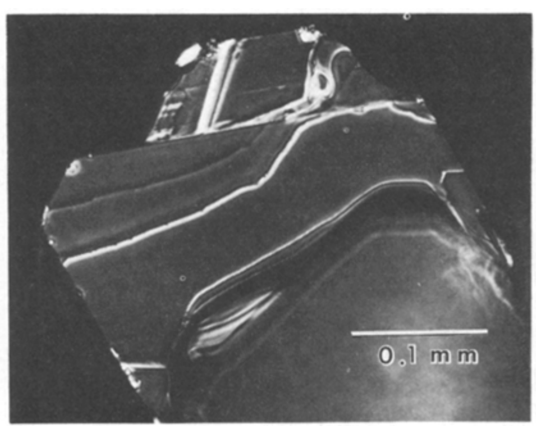

Figure 6 Positive phase-contrast photograph of the bottom surface $(0 0 0 \bar{1})$ of $20H_{(b)}$.

S_{c9}	S_{c10}	S_{c11}	S_{c12}	S_{c13}	S_{c14}	S_{c15}	S_{c16}	S_{c17}	S_{c18}
2.0	1.0	2.0	2.0	2.7	1.0	3.6	2.7	2.0	1.0
2.2	1.6	0.5	1.3	1.0	0.9	1.6	2.5	1.8	1.4
0.9	2.1	1.6	0.4	1.7	0.7	1.1	0.7	0.9	2.6
0.4	0.3	3.1	2.9	0.5	3.3	0.3	0.2	3.1	3.0
1.5	4.3	2.0	3.0	0.4	4.1	0.7	1.1	4.0	2.5
6.0	1.8	3.5	3.5	7.6	3.0	7.9	7.4	3.5	4.6
6.4	8.0	8.3	7.3	1.7	4.5	2.8	4.5	6.4	6.9
5.3	3.8	1.6	5.7	6.1	8.8	3.8	2.3	5.3	3.4
4.0	6.2	6.7	3.0	7.3	3.2	4.5	2.8	1.5	2.5
7.1	5.0	6.1	8.1	3.1	2.6	5.0	8.1	2.7	5.6
6.0	7.6	6.0	3.5	7.9	9.6	10.8	7.9	12.5	10.8
7.1	5.0	6.1	8.1	3.1	2.6	5.0	8.1	2.7	5.6
4.0	6.4	6.7	3.0	7.4	3.2	4.5	2.8	1.5	2.6
5.3	3.8	1.0	5.7	6.1	8.8	3.8	2.3	5.3	3.4
6.4	8.0	8.4	7.3	1.7	4.6	2.8	4.5	6.4	6.9
6.0	1.8	3.5	3.5	7.6	3.0	7.9	7.5	3.5	4.6
1.5	4.3	2.0	3.0	0.4	4.1	0.7	1.1	4.0	2.5
0.4	0.3	3.1	2.9	0.5	3.3	0.3	0.3	3.1	3.0
0.9	2.1	1.6	0.4	1.7	0.7	1.1	0.7	0.9	2.6
2.2	1.6	0.5	1.3	1.0	0.8	1.6	2.5	1.8	1.4
2.0	1.0	2.0	2.0	2.7	1.0	3.6	2.7	2.0	1.0
(662222)	(553223)	(552332)	(533522)	(444422)	(443333)	(44222222)	(42242222)	(33332222)	(32322323)
43.9	64.3	73.0	75.2	34.0	70.3	9.1	37.7	65.2	55.4
36.7	42.2	42.4	36.8	66.1	46.1	45.9	46.2	29.7	7.9

the X-ray diffraction pattern of $6/mmm$; nevertheless the true symmetry of crystal structure is $P\,3m1$. He gave a theoretical interpretation such that the zigzag sequence, being symmetrical along the c-axis, causes the hexagonal symmetry of $6/mmm$ on the X-ray diffraction pattern. Later, Sadanaga *et al.* [12] defined the phenomenon such that the diffraction symmetry is enhanced higher than the true symmetry of crystal structure as "diffraction enhancement of symmetry", and they investigated theoretically the diffraction enhancement of symmetry in the case of SiC polytype [14–16].

Therefore, we must also consider the possibility of the occurrence of diffraction enhancement of symmetry. In other words, the layer sequences of trigonal rather than hexagonal symmetry should be taken into consideration for the layer structure determination of $20H_{(a)}$ and $20H_{(b)}$. The possible layer sequences of 20-layered trigonal structures can also be easily derived from the "simplified method" as demonstrated in the previous paper (Part 1). There are 79 possible layer sequences of 20-layered trigonal structures [5]. These 79 possible layer sequences are presented in Table II. The S values of these 79

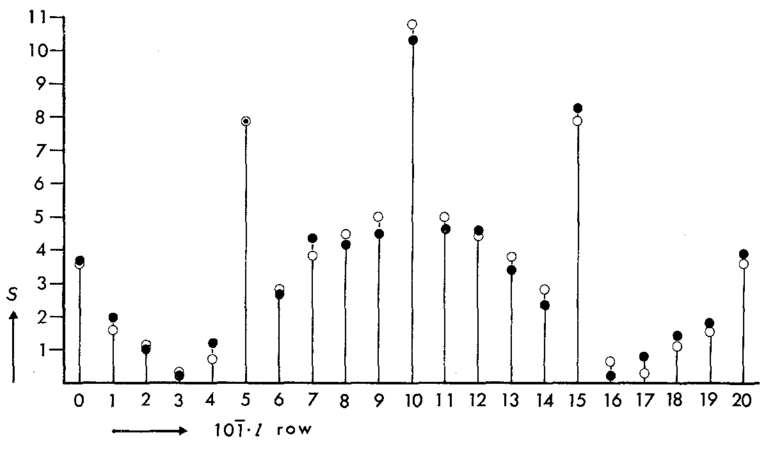

Figure 7 A graphical comparison between the calculated S_c values of (44222222) sequence (shown by open circles) and the observed S_0 values of $20H_{(a)}$ polytype (marked by dots) of the $1\,0\,\bar{1}\cdot l$ reflections.

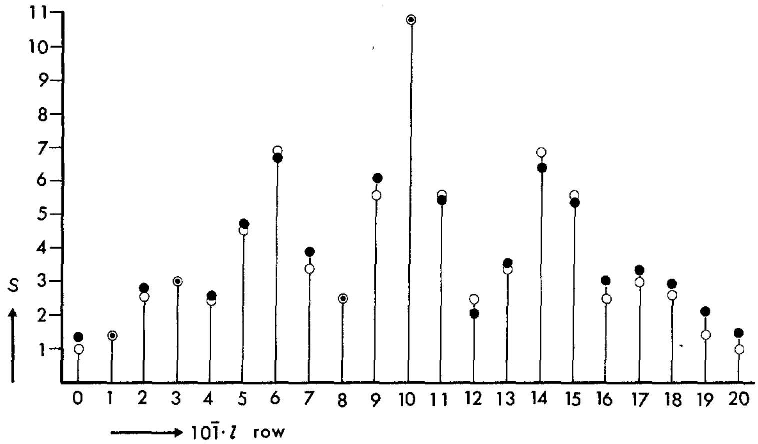

Figure 8 A graphical comparison between the calculated S_c of (32322323) sequences (shown by open circles) and the observed S_0 values of $20H_{(b)}$ polytype (marked by dots) of the $10\bar{1}\cdot l$ reflections.

sequences were also calculated. Among these 79 cases, 13 sequences which give hexagonal symmetry on the calculated diffraction pattern were chosen and their calculated S values were compared with $S_{0\cdot a}$ and $S_{0\cdot b}$ values, respectively. The values of RA_n and RB_n of these 13 sequences were also calculated. These calculated $S_{c\cdot n}$ (n ranging from 6 to 18), RA_n and RB_n values are also tabulated in Table I. As is obvious from Table I, the layer sequence of (44222222) gives a minimum RA value of 9.1%, and (32322323) a minimum RB of 7.9%. Figs. 7 and 8 show the satisfactory agreement between observed S_0 and calculated S_c for (44222222) and (32322323) layer sequences, respectively.

Thus, by applying the "simplified method" to these complex polytypes, their layer structures may easily be determined. If we had taken into account the layer sequences which include the Zhdanov number "1", we would have been confronted with 4625 possibilities [22], a very formidable task! Therefore, without making a painful detour or being misled by the phenomenon of diffraction enhancement of symmetry, we were successfully led to the solution of layer structure of $20H_{(a)}$ and $20H_{(b)}$ with the aid of the "simplified method" based on the principle of the exclusion of "1".

TABLE II 79 possible layer sequences derived by excluding those bearing the Zhdanov number "1" for a 20-layer trigonal structure

16.4, 14.222, 13.7, 13.232, 12.242, 11.522, 11.252, 11.432, 10.262, 10.532, 10.433, 9272, 9542, 9443, 932222, 922322, 8822, 8723, 8624, 8552, 8525, 8453, 833222, 832232, 823322, 7733, 7562, 7634, 7463, 7535, 734222, 732242, 724322, 723233, 723332, 6644, 662222, 6545, 635222, 632522, 632252, 632225, 652322, 625322, 642422, 642323, 634232, 633242, 642224, 632423, 624332, 553322, 553223, 552332, 535232, 525233, 522533, 534242, 543422, 543224, 542432, 524342, 543323, 542333, 532433, 444422, 443432, 444323, 443333, 44222222, 42242222, 43232222, 43222322, 43222223, 42232322, 33332222, 33322322, 33233222, 32322323.

Acknowledgement

The authors would like to express their sincere gratitude to Emeritus Professor R. Sadanaga, Mineralogical Institute, University of Tokyo for his guidance and encouragement.

References

1. A. R. VERMA and P. KRISHNA, "Polymorphism and Polytypism in Crystals" (Wiley, New York, 1966).
2. P. T. B. SCHAFFER, *Acta Cryst.* **B25** (1969) 477.
3. G. C. TRIGUNAYAT and G. K. CHADHA, *Phys. Stat. Sol.* (*a*) 4 (1971) 9.
4. Z. INOUE and Y. INOMATA, *Prog. Crystal Growth Charact.* (1982) in preparation.
5. Z. INOUE, *J. Mater. Sci.* 17 (1982) 3189.
6. Z. INOUE, Y. INOMATA and H. TANAKA, *Mineral. J.* 6 (1972) 486.
7. Z. INOUE, H. KOMATSU, H. TANAKA and Y. INOMATA, "Silicon Carbide – 1973", Proceedings of the 3rd International Conference at Florida, September 1973 (University of South Carolina Press, Columbia, South Carolina, 1973) p. 191.
8. Y. INOMATA, Z. INOUE, M. MITOMO and S. SUENO, *J. Ceram. Assoc. Japan* 77 (1969) 143.
9. Y. INOMATA and Z. INOUE, *ibid.* 78 (1970) 133.
10. P. KRISHNA, R. C. MARSHALL and C. F. RYAN, *J. Cryst. Growth* 8 (1971) 129.
11. T. TAGAI, S. SUENO and R. SADANAGA, *Mineral J.* 6 (1971) 240.
12. R. SADANAGA and H. TAKEDA, *Acta Cryst.* **B24** (1968) 144.
13. L. S. RAMSDELL and J. A. KOHN, *ibid.* 4 (1951) 111.

14. R. SADANAGA, K. OHSUMI and T. MATSUMOTO, *Proc. Japan Acad.* **49** (1973) 816.
15. *Idem, ibid.* **49** (1973) 609.
16. K. TSUKIMURA, *Kobutsu Gakkaishi* **14** (1980) 323.
17. Y. INOMATA, Z. INOUE, M. MITOMA and H. TANAKA, *J. Ceram. Assoc. Japan* 77 (1969) 83.
18. Y. INOMATA, *J. Crystal Growth* **12** (1972) 57.
19. F. C. FRANK, *Phil. Mag.* **42** (1951) 1014.
20. Y. INOMATA, M. MITOMO, Z. INOUE and H. TANAKA, *J. Ceram. Assoc. Japan* 76 (1968) 355.
21. H. TAKEDA, *Acta Cryst.* **22** (1967) 845.
22. J. E. IGLESIAS, *Z. Krist.* **155** (1981) 121.

Received 1 March
and accepted 22 March 1982